Consistent Thermodynamic Treatment of Two-Phase Interfaces in Compressible Fluid Flow

By M. Hoffmann, W. Boscheri†, M. Dumbser†, R. Saurel‡, S. Fechter, S. Keller AND C.-D. Munz

Institut für Aerodynamik und Gasdynamik, Universität Stuttgart
Pfaffenwaldring 21, 70569 Stuttgart

A pressure-based diffuse interface scheme for the simulation of compressible flows with phase transition is presented and assessed with the help of a one-dimensional test case. In this context, the energy equation is reformulated in terms of pressure and kinetic energy establishing the pressure-based character of the approach. The method is able to handle compressible flows as accurate results are obtained for a standard one-dimensional shock tube test case. In this contribution, we use a thermodynamic equilibrium relaxation method which is in consistency with the second law of thermodynamics. The approach is applied to a problem characterized by a large initial density and pressure jump, which produces phase transition.

1. Introduction

Due to the fact that in a compressible multi-phase fluid flow the interface behavior is directly coupled to the fluid flow, the numerical modeling of these flows is rather cumbersome. There are two main approaches in the direct simulation of two-phase flow: Diffuse interface and sharp interface methods. In the diffuse interface approach the interface is allowed to be smeared out over a few grid cells as it is usually done by shock-capturing schemes. Due to the numerical smearing, states at the interface occur which are non-physical and an appropriate numerical modeling of the thermodynamic behavior is needed to guarantee that the numerical results cover the physics. Examples for such an approach are phase field models and the Baer-Nunziato approach as multi-fluid model.
In contrast to this, the sharp interface approach tries to keep the interface sharp in a way such that no non-physical value occurs. For this purpose an interface tracking like the level-set approach or a marker particle method is needed. Alternatively a moving grid can be used. The interface tracking schemes have then to be combined with a sub-cell resolution or a ghost-fluid method to keep the interface sharp.

In the field of computational fluid dynamics there are two well-established concepts of flow simulation algorithms that are called pressure- and density-based methods. While

† Laboratory of Applied Mathematics
Department of Civil, Environmental and Mechanical Engineering, University of Trento
Via Mesiano 77, 38123 Trento, Italy
‡ Polytech Marseille, Aix-Marseille University, UMR CNRS 6595 IUSTI
5 rue E. Fermi, 13453 Marseille Cedex 13, FranceEcole d'ingénieurs d'Aix-Marseille Université

pressure-based approaches are widely used to simulate hydrodynamic flows on the basis of the incompressible flow equations, the density-based schemes can be considered to be the standard methods for compressible flows. Both approaches are distinguished by the use of pressure and density as primary variable, respectively. Although the requirements for the simulation of compressible and incompressible flows differ considerably, a lot of effort has been put into efficiently accessing the weakly compressible regime with both methods. For this purpose, so-called preconditioning techniques are used e.g. for the density-based approaches. On the other hand, the originally pressure-based methods can also be extended to the compressible flow regime.

One possibility for extending a pressure-based incompressible algorithm to the compressible regime is the so-called multiple pressure variables (MPV) approach proposed by Munz *et al*. [1,2]. The method builds upon a pressure decomposition in dependency of a global flow Mach number. In this context, the conservative energy equation is reformulated in terms of pressure and kinetic energy. Therefore, the total energy is first split in its internal and kinetic part. Afterwards, the internal energy is replaced with the help of an equation of state (EOS). Finally, the numerical algorithm includes the solution of a pressure Poisson equation, similar to classical incompressible schemes.

In the following we apply the MPV approach to a reduced Baer-Nunziato model of Saurel *et al*. [3] where a mixture stiffened gas equation is used as EOS. The phase change is calculated with a pressure, temperature and Gibbs free energy equilibrium relaxation solver by LeMartelot *et al*. [4] which is in agreement with the second law of thermodynamics.

The outline of the report is as follows. In the first section, the governing equations for the numerical simulation are introduced. This is followed by the introduction of the relaxation solver. In the following section, the results of a two-phase shock tube with and without phase transition [3] are shown.

2. Governing equations

In this section we describe the equations that are used for the numerical simulations with the pressure-based method.

2.1. *Compressible Two-Phase Flow System*

The equations for volume fraction, mass, momentum and total energy for inviscid flows without gravitational and external forces and heat conduction in compressible gas dynamics are given by the reduced Baer-Nunziato equations:

$$\frac{\partial \alpha_1}{\partial t} + \mathbf{u} \cdot \nabla \alpha_1 = \overbrace{\frac{\alpha_1 \alpha_2 \left(\rho_2 c_2^2 - \rho_1 c_1^2\right)}{\alpha_2 \rho_1 c_1^2 + \alpha_1 \rho_2 c_2^2}}^{K_{\alpha_1}} \nabla \cdot \mathbf{u}, \tag{2.1}$$

$$\frac{\partial \alpha_1 \rho_1}{\partial t} + \nabla \cdot (\alpha_1 \rho_1 \mathbf{u}) = 0, \tag{2.2}$$

$$\frac{\partial \alpha_2 \rho_2}{\partial t} + \nabla \cdot (\alpha_2 \rho_2 \mathbf{u}) = 0, \tag{2.3}$$

$$\frac{\partial \rho \mathbf{u}}{\partial t} + \nabla \cdot [(\rho \mathbf{u}) \circ \mathbf{u}] + \nabla p = 0, \tag{2.4}$$

$$\frac{\partial \rho E}{\partial t} + \nabla \cdot [\mathbf{u} (\rho E + p)] = 0. \tag{2.5}$$

Here α_k denotes the volume fraction of each phase, ρ_k the density and c_k the speed of sound. The vector $\mathbf{u}$ stands for the velocities, which has only one entry for 1D-calculations. ρ denotes the mixture density ($\alpha_1\rho_1 + \alpha_2\rho_2$), p the pressure. The total energy is given by

$$\rho E = \rho e + 1/2 \rho \mathbf{u}^2, \tag{2.6}$$

where e is the internal energy. The mixture pressure is derived from the two stiffened-gas equations of the two phases

$$p = \frac{\rho (e - Y_1 q_1 - Y_2 q_2) - \left(\frac{\alpha_1 \gamma_1 p_{\infty,1}}{\gamma_1 - 1} + \frac{\alpha_2 \gamma_2 p_{\infty,2}}{\gamma_2 - 1}\right)}{\frac{\alpha_1}{\gamma_1 - 1} + \frac{\alpha_2}{\gamma_2 - 1}}, \tag{2.7}$$

with $Y_k = \alpha_k \rho_k / \rho$ and $q_k, p_{\mathrm{inf},k}, \gamma_k$ denoting parameters for each phase.
Reorganize (2.7) to ρe, inserting this into (2.6) and the result in the energy equation (2.5) leads to the equation

$$\begin{aligned} \frac{\partial p}{\partial t} = & -\frac{(1+\beta)}{\beta} \nabla \cdot (p \mathbf{u}) - \frac{1}{\beta} \left(\frac{\partial e_{\mathrm{kin}}}{\partial t} + \nabla \cdot (e_{\mathrm{kin}} \mathbf{u}) \right) \\ & - \frac{\gamma_1 p_{\infty,1}}{\beta(\gamma_1 - 1)} \left(\frac{\partial \alpha_1}{\partial t} + \nabla \cdot (\alpha_1 \mathbf{u}) \right) - \frac{\gamma_2 p_{\infty,2}}{\beta(\gamma_2 - 1)} \left(\frac{\partial \alpha_2}{\partial t} + \nabla \cdot (\alpha_2 \mathbf{u}) \right) \\ & - \frac{p}{\beta} \left(\frac{1}{\gamma_1 - 1} - \frac{1}{\gamma_2 - 1} \right) \left(\frac{\partial \alpha_1}{\partial t} + \mathbf{u} \cdot \nabla \alpha_1 \right), \end{aligned} \tag{2.8}$$

where β is defined by

$$\beta = \left(\frac{\alpha_1}{\gamma_1 - 1} + \frac{\alpha_2}{\gamma_2 - 1} \right).$$

For the MPV approach a pressure splitting is introduced which is knows as

$$p = p^{(0)} + M^2 p^{(2)},$$

where $\nabla p^{(0)} = 0$.

The final non-dimensional equation system reads as

$$
\begin{aligned}
&\frac{\partial \alpha_1}{\partial t} + \mathbf{u} \cdot \nabla \alpha_1 = \mathsf{K}_{\alpha_1} \nabla \cdot \mathbf{u}, \\
&\frac{\partial \alpha_1 \rho_1}{\partial t} + \nabla \cdot (\alpha_1 \rho_1 \mathbf{u}) = 0, \\
&\frac{\partial \alpha_2 \rho_2}{\partial t} + \nabla \cdot (\alpha_2 \rho_2 \mathbf{u}) = 0, \\
&\frac{\partial \rho \mathbf{u}}{\partial t} + \nabla \cdot \left[(\rho \mathbf{u}) \circ \mathbf{u} \right] + \nabla p^{(2)} = 0, \\
&M^2 \frac{\partial p^{(2)}}{\partial t} = -\frac{\partial p^{(0)}}{\partial t} - \frac{(1+\beta)}{\beta} \nabla \cdot (p \mathbf{u}) \\
&- \frac{M^2}{\beta} \left(\frac{\partial e_{\mathsf{kin}}}{\partial t} + \nabla \cdot (e_{\mathsf{kin}} \mathbf{u}) \right) \\
&- \frac{\gamma_1 p_{\infty,1}}{\beta(\gamma_1 - 1)} \left(\frac{\partial \alpha_1}{\partial t} + \nabla \cdot (\alpha_1 \mathbf{u}) \right) - \frac{\gamma_2 p_{\infty,2}}{\beta(\gamma_2 - 1)} \left(\frac{\partial \alpha_2}{\partial t} + \nabla \cdot (\alpha_2 \mathbf{u}) \right) \\
&- \frac{p}{\beta} \left(\frac{1}{\gamma_1 - 1} - \frac{1}{\gamma_2 - 1} \right) \left(\frac{\partial \alpha_1}{\partial t} + \mathbf{u} \cdot \nabla \alpha_1 \right).
\end{aligned}
\tag{2.9}
$$

A parameter called global flow Mach number M is introduced in the above equations, which comes from the nondimensionalization. The global flow Mach number results from the choice of different reference values for the speed of sound and the fluid velocity:

$$M = \frac{|\mathbf{v}_{ref}|}{\sqrt{p_{ref}/\rho_{ref}}}.$$

For the calculations shown in this report $M = 1$.

3. Relaxation Solvers

For the phase change calculations, two approaches are suitable for the MPV-Baer-Nunziato solver. Both approaches consider thermodynamic equilibrium in agreement with the second law of thermodynamics. The so called stiff thermo-chemical solver is explained by Saurel *et al*. [3] and solves a system of ordinary differential equations. The other approach proposed by LeMartelot *et al*. [4] solves a zero function to obtain the thermodynamic equilibrium.
Since the later is more robust, it was chosen to be used in the MPV solver and will be explained in more detail in the following subsection.

3.1. *Thermodynamic relaxation solver*

The system (2.9) solves the flow mixture for mechanical and thermal equilibrium but not for thermodynamic equilibrium. To get thermodynamic equilibrium only in a vapor-liquid mixture a interface criterion is considered

$$\alpha_1 \in [\epsilon, 1 - \epsilon]. \tag{3.1}$$

In this mixture zone the thermodynamical equilibrium state is determined by the following definitions (subscript 1 is for the liquid state and 2 for the vapor):

$$\begin{aligned} v &= \frac{1}{\rho} = Y_1 v_1 + Y_2 v_2 = \text{const.} = v_0, \\ e &= Y_1 e_1 + Y_2 e_2 = \text{const.} = e_0, \\ T_1 &= T_2 = T, \\ p_1 &= p_2 = p, \\ g_1 &= g_2. \end{aligned} \tag{3.2}$$

When the relaxed state is denoted by '$*$' the volume equation becomes

$$v_0 = Y_1^* v_1^*(p^*, T^*) + (1 - Y_1^*) v_2^*(p^*, T^*). \tag{3.3}$$

With the constraints of System (3.2) for pressures, temperatures and Gibs free energies the final temperature T^* becomes the saturation temperature $T_{\text{Sat}}(p^*)$. In this approach the saturation curve is obtained from the EOS proposed by Lemmon and Huber [5]. A polynomial representation of that curve is used in this implementation to avoid high computational cost. Now a first linking of the liquid mass fraction and the final state pressure is obtained by

$$Y_1^* = \frac{v_2^*(p^*) - v_0}{v_2^*(p^*) - v_1^*(p^*)}. \tag{3.4}$$

The second linking is obtained with the constraint that the energy is constant

$$e_0 = Y_1^* e_1^*(p^*, T^*) + (1 - Y_1^*) e_2^*(p^*, T^*). \tag{3.5}$$

Since both linkings must be true a single equation must be solved

$$\frac{e_2^*(p^*) - e_0}{e_2^*(p^*) - v_1^*(p^*)} - \frac{v_2^*(p^*) - v_0}{v_2^*(p^*) - v_1^*(p^*)} = 0. \tag{3.6}$$

The solution of equation (3.6) is computed with the bisection method. For further and a more detailed explanation see [3] and [4].

4. Test case and Results

4.1. *Test case*

A detailed description of the test case can be found in [3]. A vertical tube is filled with one fluid, a membrane separates the liquid from a very low pressure vapor chamber of this fluid. As soon as the membrane is destroyed a rarefaction front runs through the liquid producing a superheated liquid behind it. Behind that front through the superheated liquid propagates a phase-transition front producing a liquid-vapor mixture. In Fig. 1 the initial state and a state during the wave propagation is shown.

4.2. *Results*

4.2.1. *Two-phase shock tube without mass transfer*

The fluid used in this example is dodecane. A 1m tube is filled with liquid dodecane in the left part. The pressure of the liquid is $p_l = 10^8$ Pa and the density is $\rho_l = 500$kg m^{-3}. The membrane is located at $x = 0.75$m. The right part is filled with dodecane vapor with a pressure of $p_r = 10^5$ Pa and a density of $\rho_r = 2$kg m^{-3}. α_1 and α_2 are initially set to 10^{-8}

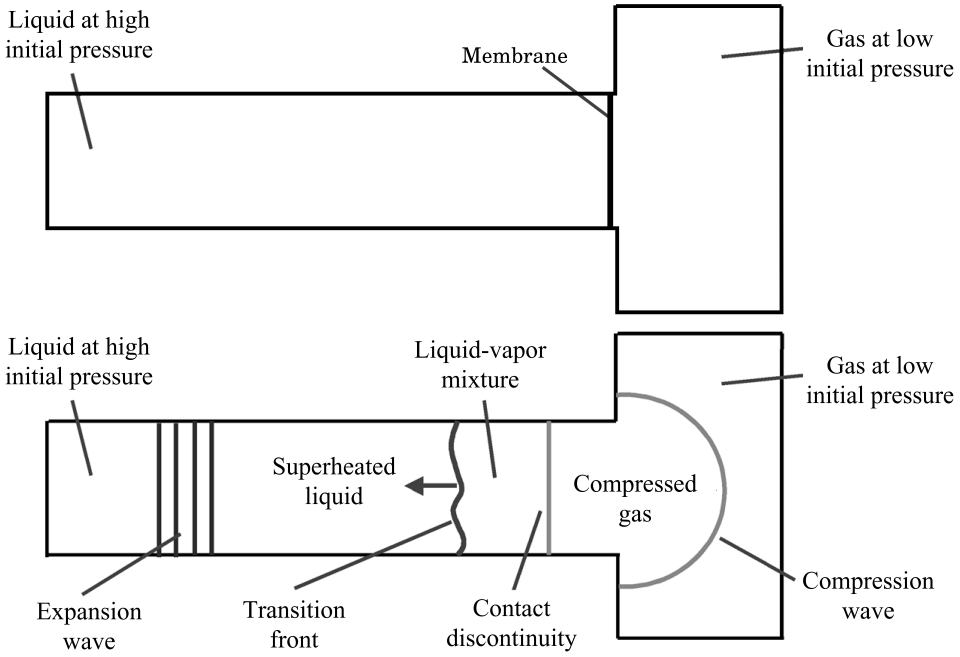

FIGURE 1. **Top**: the initial state of the tube. **Bottom**: the membrane is ruptured and the waves of a cavitating system propagating through the tube.

for numerical reason. This test does not include the relaxation solver, which means, that no phase transition can occur. The end time is $t = 473\mu s$. In Fig. 2 the numerical result shows a good agreement with the exact solution.

4.2.2. *Two-phase shock tube with mass transfer*

For this test case the same setup as in section 4.2.1 is used, but this time with the relaxation solver. The epsilon for the interface is chosen to $\epsilon = 10^{-2}$. The extra evaporation wave appears in Fig. 3. The second jump in the vapor mass fraction is the contact discontinuity between the liquid-vapor mixture produced by evaporation.

5. Conclusion

The MPV-approach is used to transfer the density-based diffuse interface approach from Saurel *et al.* [3] to a pressure-based system. A suitable thermodynamic equilibrium relaxation solver from LeMartelot *et al.* [4] is used to calculate the phase transition with the MPV-solver. Without mass exchange the solver shows good agreement with the exact solution. If phase transition is allowed by using the relaxation solver at the interface, an evaporation front appears in the numerical solutions. Compared to the results from [3] the plots are quite similar. The biggest differences are in the evaporation front velocity and in the vapor mass fraction. These difference need to be further investigated in the future.

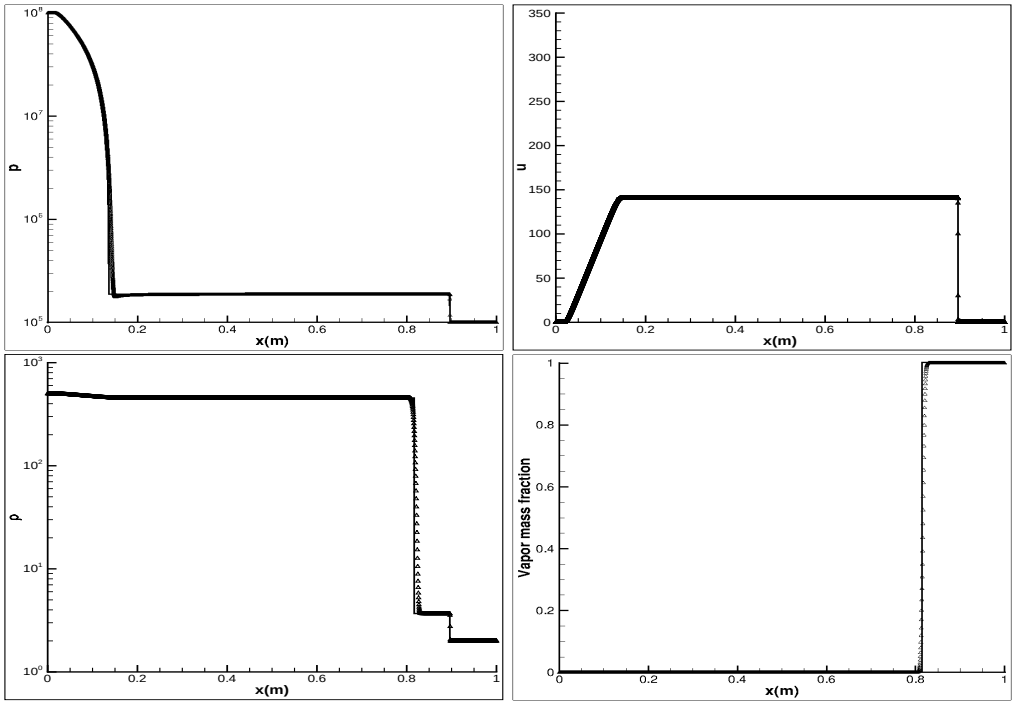

FIGURE 2. The liquid-vapor shock tube filled with dodecane but without phase transition. The symbols represent the numerical solution, the solid lines show the exact one.

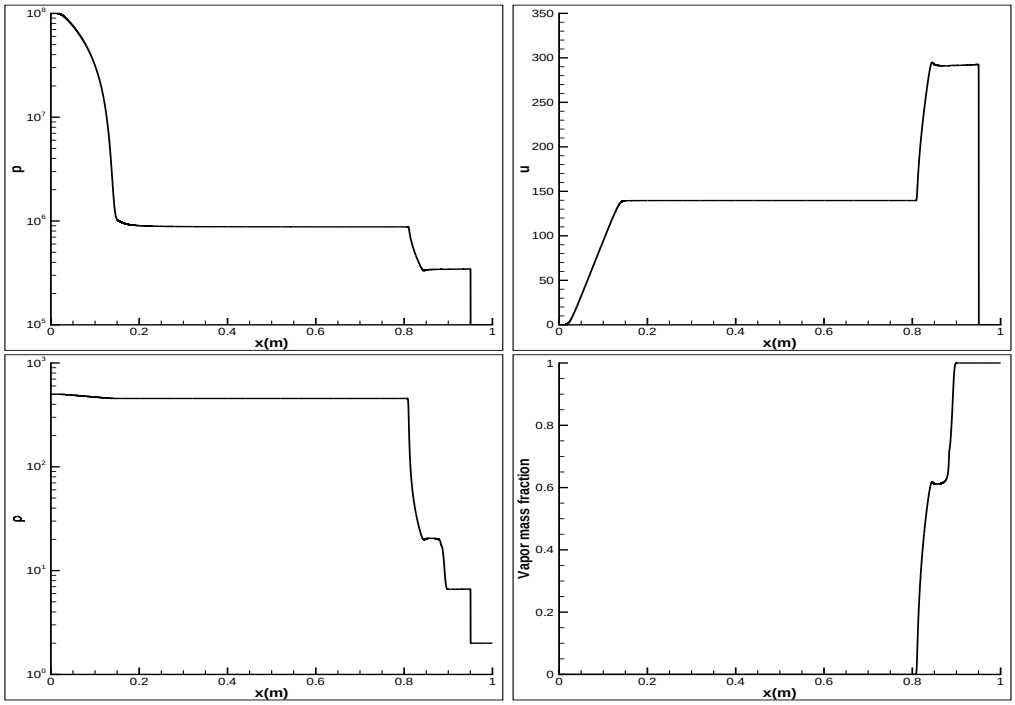

FIGURE 3. Here the same initial setup is used as in Fig. 2 but here the relaxation solver for phase change is used at the interface. The line represents the numerical result.

Acknowledgments

Financial support has been provided by the German Research Foundation (Deutsche Forschungsgemeinschaft – DFG) in the framework of the Sonderforschungsbereich Transregio 40 and the IGSSE (International Graduate School of Science and Engineering) at the TU München.

References

[1] MUNZ, C.-D., ROLLER, S., KLEIN, R., GERATZ, K. J. AND REITZ, R. D. (2003). The extension of incompressible flow solvers to the weakly compressible regime. *Computers & Fluids*, **32**(2), 173–196.

[2] PARK, J. H. AND MUNZ, C.-D. (2005). Multiple pressure variables methods for fluid flow at all Mach numbers. *International Journal for Numerical Methods in Fluids*, **49**, 905–931.

[3] R. SAUREL, PETITPAS, F. AND ABGRALL, R. (2008). Modelling phase transition in metastable liquids: application to cavitating and flashing flows. *J. Fluid Mech.*, **607**, 313–350.

[4] LEMARTELOT, S., NKONGA, B. AND SAUREL, R. (2013). Liquid and liquid-gas flows at all speeds. *J. Comp. Phys.*, **255**, 53–82.

[5] LEMMON, E. W. AND HUBER, M. L. (2004). Thermodynamic properties of n-dodecane. *Energy & Fuels*, **18**, 960–967.